Received: 22 February 2021 | Revised: 10 June 2021 | Accepted: 10 June 2021

DOI: 10.1111/cas.15025

ORIGINAL ARTICLE

Cancer Science WILEY

Oxytocin receptor is a promising therapeutic target of malignant mesothelioma

Yuta Kodama[1] | Ichidai Tanaka[1] | Tatsuhiro Sato[2] | Kazumi Hori[1] | Soei Gen[1] | Masahiro Morise[1] | Daisuke Matsubara[3] | Mitsuo Sato[4] | Yoshitaka Sekido[2,5] | Naozumi Hashimoto[1]

[1]Department of Respiratory Medicine, Nagoya University Graduate School of Medicine, Nagoya, Japan

[2]Division of Cancer Biology, Aichi Cancer Center Research Institute, Nagoya, Japan

[3]Department of Diagnostic Pathology, Tsukuba University, Tsukuba, Japan

[4]Department of Pathophysiological Laboratory Sciences, Nagoya University Graduate School of Medicine, Nagoya, Japan

[5]Department of Molecular and Cellular Oncology, Nagoya University Graduate School of Medicine, Nagoya, Japan

Correspondence
Ichidai Tanaka, Department of Respiratory Medicine, Nagoya University Graduate School of Medicine, 65 Tsurumai-cho, Showa-ku, Nagoya 466-8550, Japan.
Email: ichidai@med.nagoya-u.ac.jp

Funding information
This research was supported by Grant-in-Aid for Scientific Research (B) 20H03689 from the Japan Society for the Promotion of Science, AMED under Grant Number (JP 20lm0203005j0004) and the Nitto Foundation for I. Tanaka.

Abstract

Malignant mesothelioma (MM) is one of the most aggressive tumors. We conducted bioinformatics analysis using Cancer Cell Line Encyclopedia (CCLE) datasets to identify new molecular markers in MM. Overexpression of oxytocin receptor (*OXTR*), which is a G-protein–coupled receptor for the hormone and neurotransmitter oxytocin, mRNA was distinctively identified in MM cell lines. Therefore, we assessed the role of *OXTR* and its clinical relevance in MM. Kaplan-Meier and Cox regression analyses were applied to assess the association between overall survival and *OXTR* mRNA expression using The Cancer Genome Atlas (TCGA) datasets. The function of *OXTR* and the efficacy of its antagonists were investigated in vitro and in vivo using MM cell lines. Consistent with the findings from CCLE datasets analysis, *OXTR* mRNA expression was highly increased in MM tissues compared with other cancer types in the TCGA datasets, and MM cases with high *OXTR* expression showed poor overall survival. Moreover, *OXTR* knockdown dramatically decreased MM cell proliferation in cells with high *OXTR* expression via tumor cell cycle disturbance, whereas oxytocin treatment significantly increased MM cell growth. *OXTR* antagonists, which have high selectivity for OXTR, inhibited the growth of MM cell lines with high *OXTR* expression, and oral administration of the *OXTR* antagonist, cligosiban, significantly suppressed MM tumor progression in a xenograft model. Our findings suggest that *OXTR* plays a crucial role in MM cell proliferation and is a promising therapeutic target that may broaden potential therapeutic options and could be a prognostic biomarker of MM.

KEYWORDS

G1 phase cell cycle checkpoints, G-protein–coupled receptors, malignant mesothelioma, oxytocin receptor, oxytocin receptor antagonists

Abbreviations: BAP1, BRCA1-associated protein-1; CCLE, Cancer Cell Line Encyclopedia; CDKN2A, cyclin-dependent kinase inhibitor 2A; FCS, fetal calf serum; IL, interleukin; LATS2, large tumor suppressor kinase 2; MM, malignant mesothelioma; NF2, neurofibromin 2; OXT, oxytocin; OXTR, oxytocin receptor; qRT-PCR, quantitative real-time polymerase chain reaction; SETD2, SET domain containing 2; TCGA, The Cancer Genome Atlas; TP53, tumor protein p53; YAP1, Yes-associated protein 1.

1 | INTRODUCTION

Malignant mesothelioma (MM) arises from mesothelial cells and is a highly aggressive neoplasm that is usually associated with long-term exposure to asbestos.[1,2] The number of global annual deaths has been approximately 40 000 people in recent years, and the incidence of MM is still increasing in Eastern Europe and some Asian countries where asbestos has not been banned or where bans have been delayed.[1,3] Most patients are diagnosed at advanced stages due to nonspecific and late symptoms, and the median survival time is 10-15 months after diagnosis.[4,5] MM is intrinsically resistant to cytotoxic chemotherapy, and the response rate to a standard chemotherapy of cisplatin/carboplatin and pemetrexed for MM is 18.6%-41.3%.[6,7] In October 2020, the Food and Drug Administration approved the combined use of nivolumab plus ipilimumab as a first-line treatment for adult patients with unresectable MM. Its therapeutic effect has been recognized in some patients, and the median progression-free survival and overall response rate were 6.8 months and 40%, respectively.[8-10]

Molecular genetic analyses have identified several fundamental genetic alterations that are responsible for the MM development. Primal genetic alterations have been characterized as frequent inactivators of tumor suppressors, such as *cyclin-dependent kinase inhibitor 2A* (*CDKN2A*), *BRCA1-associated protein-1* (*BAP1*), and *neurofibromin 2* (*NF2*).[11,12] Copy number loss and recurrent somatic mutations in these genes are related to cell cycle abnormalities, histone oncomodifications, and disorder of multiple signaling cascades, including the Hippo signaling and mammalian target of rapamycin pathways.[13,14] We previously identified frequent inactivation of the component molecules of the Hippo signaling pathway that control organ size through regulation of cell proliferation and apoptosis.[15-17] Dysfunction of the Hippo signaling pathway constitutively activates the transcriptional coactivator, Yes-associated protein 1 (YAP1), and promotes the expression of several target genes;[18,19] however, no targeted therapies exploiting these genetic alterations have emerged. Therefore, it is essential to establish new promising therapeutic strategies against MM.

We analyzed genes that were highly expressed in MM cell lines compared with other types of cancer cell lines using the Cancer Cell Line Encyclopedia (CCLE) dataset to identify new therapeutic targets in MM. *Oxytocin receptor* (*OXTR*), which is a G-protein–coupled receptor, was identified as a gene that was markedly increased in MM cell lines. *OXTR* acts as a receptor for oxytocin (OXT), which is a peptide hormone released by the posterior pituitary that plays a role in milk secretion and uterine contraction during labor.[20] An association between OXT-OXTR signaling and tumor development has been indicated in some cancer types.[21,22] We further investigated the role of OXT-OXTR signaling in MM using knockdown experiments and *OXTR* antagonists.

2 | MATERIALS AND METHODS

2.1 | *Cell culture*

Nine Japanese MM cell lines including ACC-MESO-1, -4, Y-MESO-22, -27, -28, -30, -37, -45, and -72, were established in our laboratory, and cells at 10-15 passages were used for each assay.[15] Five MM cell lines, including NCI-H28, NCI-H2052, NCI-H2373, NCI-H2452 and MSTO-211H, and MeT-5A (an immortalized mesothelial cell line), were purchased from the American Type Culture Collection. Cell line authentication of NCI-H2052, NCI-H2373, NCI-H2452, and MeT-5A cells was performed using short tandem repeat analysis. All MM cell lines and MeT-5A cells were maintained in RPMI-1640 culture medium (Sigma-Aldrich) containing 5% fetal calf serum (FCS) in an atmosphere of 5% CO_2 and 95% air at 37°C. 293FT cells were cultured in DMEM (Thermo Fisher Scientific) supplemented with 5% FCS.

2.2 | *Short-hairpin RNA (shRNA) expression*

For lentivirus production, 293FT cells were transfected with three plasmids: pMD2.G (Plasmid #12259; addgene), psPAX2 (Plasmid #12260; addgene), and sh*OXTR* (using pLKO.1 puro [Plasmid #8453; addgene])/scramble shRNA (Plasmid #1864; addgene). Transfections were performed using X-tremeGENE HP DNA Transfection Reagent (#6366236001; Merck), and scrambled shRNA was used as control. The following sh*OXTR* sequences were used: 5′-CCGGATCACGCTAGCTGTCTACATCCTCGAGGATGTAGACAGCTAGCGTGATTTTTTG-3′ (sh*OXTR* #1), 5′-CCGGGTAATTTCACTCCAGTATATTCTCGAGAATATACTGGAGTGAAATTACTTTTTG-3′ (sh*OXTR* #2), and 5′-CCGGGGACATCACCTTCCGCTTCTACTCGAGTAGAAGCGGAAGGTGATGTCCTTTTTG-3′ (sh*OXTR* #3). Three different shRNAs targeting *OXTR* were tested to minimize the possibility of off-target effects, and the two shRNAs with the most efficient knockdown (sh*OXTR* #1 and #2) were selected for the experiments. Lentiviruses were harvested at 48 and 96 hours after transfection. The virus concentration protocol used was described elsewhere.[23-26] Virus was frozen at −80°C in appropriately sized aliquots for infection. Y-MESO-27, NCI-H2052, or NCI-H2373 cells were seeded on plastic dishes 24 hours prior to infection. When cells reached 30%-50% confluency, they were transduced with pLKO.1-control or pLKO1-*OXTR*–knockdown lentivirus in the presence of 8 μg/mL polybrene for 24 hours. The virus was removed after the infection and replaced with fresh cell culture medium. Transduced cells were selected using 2 μg/mL puromycin for 48 hours. Selected cells were then replated (Y-MESO-27 and NCI-H2052 at a density of 5.0×10^5 cells/well; NCI-H2373 at a density of 1.0×10^6 cells/well) in 100-mm dishes. After 36 hours, the cells were harvested for RNA isolation and quantitative real-time polymerase chain reaction (qRT-PCR) analysis.

2.3 | In vivo xenograft mouse study

NCI-H2052 or NCI-H2373 cells were infected with lentiviral vectors encoding sh*OXTR* #1 or scrambled shRNA. Six-to-eight-week-old female BALB/c nude (nu/nu) mice were purchased from Charles River Laboratories Japan, Inc. For subcutaneous tumor models, mice were injected in the left buttock with 1.5×10^6 shScramble or sh*OXTR*

NCI-H2052/H2373 cells suspended in 200 μL of PBS. After 28 days, mice were euthanized with CO_2, tumors were collected, and weights were measured.

To examine antitumor efficacy of cligosiban in vivo, 6-to-8-week-old female BALB/c nude (nu/nu) mice were injected in the left buttock with 5.0×10^6 NCI-H2052 cells suspended in 200 μL of PBS. After subcutaneous administration, mice were randomized into two groups and treated with either vehicle (dimethyl sulfoxide) or 60 mg/kg cligosiban via oral administration every other day. One week after 10 doses of cligosiban, mice were euthanized with CO_2, tumors were collected, and weights were measured.

All protocols for the mouse experiments were approved by the Nagoya University Institutional Animal Care and Use Committee.

2.4 | *Statistical analysis*

Categorical data were compared using Fisher's exact test. Continuous variables were compared using the Mann-Whitney U test or unpaired *t*-test. Pearson's correlation was applied to assess the linear association between two variables. Survival analysis was performed using an independent gene expression dataset of 85 MM cases from The Cancer Genome Atlas (TCGA; http://cancergenome.nih.gov/) using Kaplan-Meier survival curves. Log-rank test was used to evaluate the statistical significance of differences of survival curves. Overall survival was defined as the time from the initial pathologic diagnosis to the date of death or last follow-up, at which point the data were censored.[27] Cox proportional hazards model analyses were performed to adjust for covariates of statistical significance in the univariate analysis, including sex, age, histology, stage, and *OXTR* mRNA expression, and to estimate the relative hazard of mortality over the follow-up period. Statistical analyses were conducted using IBM SPSS version 27 software and JMP pro 15 software. A two-sided statistical significance level of 0.05 was used for all statistical analyses.

Detailed methods for transfection with siRNA, RNA isolation, qRT-PCR analysis, cell cycle analysis, cell proliferation analysis, colony formation assay, wound-healing assay, and drug sensitivity assay are described in the supplementary materials (Appendix S1).

3 | RESULTS

3.1 | *OXTR* is highly expressed in MM and associated with poor prognosis

We analyzed genes that were highly expressed in MM cell lines (n = 11) compared with other types of cancer cell lines (n = 1008) using the CCLE datasets. We examined the expression ratio of each gene in MM cell lines compared with other cancer cell lines and found that the ratio of *OXTR* was the highest in the CCLE datasets (Table S1). *OXTR* mRNA expression was significantly higher in MM cell lines than that in other cancer cell lines ($P < .001$, Mann-Whitney *U* test) (Figure 1A) and was the highest in 25 tumor types (Figure 1B).

Moreover, we examined *OXTR* mRNA expression using the TCGA dataset to determine the clinical significance of *OXTR* expression in MM. The level of *OXTR* mRNA expression was significantly higher in MM tissue than in almost all normal tissues, except the mammary gland, and was the highest in a total of 37 tumor types, in accordance with the results of the CCLE data analysis (Figure S1A). *OXTR* mRNA expression in approximately 33.3% of MM cases was 100 times higher than that of the lowest case (Figure 1C). Therefore, we divided the 87 cases into three groups according to *OXTR* mRNA expression level: low (n = 29), moderate (n = 29), and high (n = 29) groups. Clinical and molecular biological characteristics of the 87 MM cases from TCGA datasets are summarized in Figure 1C and Table S2. Although no statistical differences were found between clinical features (sex, age, histology, and stage) and *OXTR* mRNA expression, biphasic types were less common in the low-*OXTR* group, and both cases of sarcomatoid type belonged to the high-*OXTR* group (Figure 1C and Table S2). Analysis of the molecular biological characteristics, which included frequently inactivated driver genes in MM such as *BAP1*, *NF2*, *tumor protein p53* (*TP53*), *large tumor suppressor kinase 2* (*LATS2*), and *SET domain containing 2* (*SETD2*), revealed that *OXTR* mRNA expression was statistically higher in cases with *NF2* inactivation than in those with intact *NF2* (Figure 1C and Figure S1B). Kaplan-Meier analysis revealed that the overall survival curves were clearly divided according to *OXTR* expression levels, and high expression was significantly associated with worse overall survival ($P < .001$, log-rank test) (Figure 1D). Univariate Cox regression analysis revealed that histological classification and *OXTR* mRNA expression were statistically associated with overall survival, and multivariable Cox regression analysis indicated that *OXTR* mRNA expression was the strongest independent predictor of overall survival (hazard ratio for death, 2.2; 95% confidence interval, 1.60-3.07; $P < .001$) (Table 1).

3.2 | Analysis of *OXTR* function in MM

We analyzed *OXTR* mRNA expression across our 14 MM cell lines compared with MeT-5A by qRT-PCR, and found that the expression level was >30 times higher in seven out of 14 MM cell lines compared with MeT-5A cells (Figure 2A). Therefore, we classified the seven MM cell lines as the high-*OXTR* group and the other seven as the low-*OXTR* group. We previously analyzed frequently inactivated driver genes in MM cell lines, including *BAP1*, *NF2*, *TP53*, and *LATS2*, and found that most of the MM cell lines with *NF2* inactivation were in the *OXTR*-high group, while other alterations of driver genes were not associated with *OXTR* expression levels (Table S3). These results were consistent with the findings from the analysis of TCGA dataset (Figure S1B). To investigate whether *NF2* affects *OXTR* expression, we conducted *NF2* knockdown using two *NF2*-intact MM

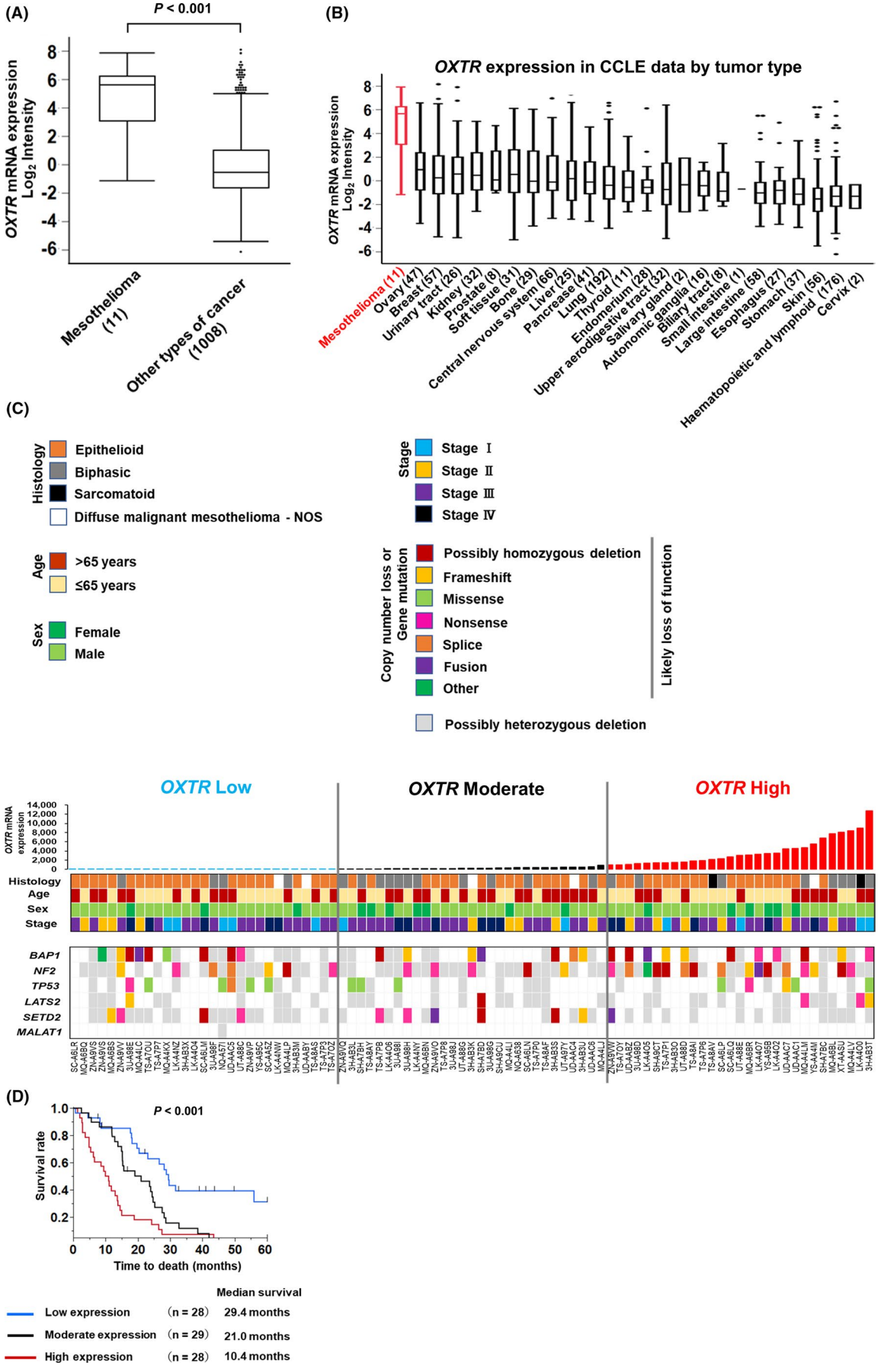
(A)
P < 0.001
OXTR mRNA expression Log2 Intensity
Mesothelioma (11)
Other types of cancer (1008)
(B)
OXTR expression in CCLE data by tumor type
OXTR mRNA expression Log2 Intensity
Mesothelioma (11)
Ovary (47)
Breast (57)
Urinary tract (26)
Kidney (32)
Prostate (8)
Soft tissue (31)
Bone (29)
Central nervous system (66)
Liver (25)
Pancreas (41)
Lung (192)
Thyroid (11)
Endometrium (28)
Upper aerodigestive tract (32)
Salivary gland (2)
Autonomic ganglia (16)
Biliary tract (8)
Small intestine (1)
Large intestine (58)
Esophagus (27)
Stomach (37)
Skin (56)
Haematopoietic and lymphoid (176)
Cervix (2)
(C)
Histology
Epithelioid
Biphasic
Sarcomatoid
Diffuse malignant mesothelioma - NOS
Age
>65 years
≤65 years
Sex
Female
Male
Stage
Stage Ⅰ
Stage Ⅱ
Stage Ⅲ
Stage Ⅳ
Copy number loss or Gene mutation
Possibly homozygous deletion
Frameshift
Missense
Nonsense
Splice
Fusion
Other
Likely loss of function
Possibly heterozygous deletion
OXTR Low
OXTR Moderate
OXTR High
OXTR mRNA expression
Histology
Age
Sex
Stage
BAP1
NF2
TP53
LATS2
SETD2
MALAT1
(D)
P < 0.001
Survival rate
Time to death (months)
Median survival
Low expression (n = 28) 29.4 months
Moderate expression (n = 29) 21.0 months
High expression (n = 28) 10.4 months

FIGURE 1 Oxytocin receptor *(OXTR)* is highly expressed in malignant mesothelioma (MM) and associated with poor prognosis. A, *OXTR* mRNA expression in MM cell lines (n = 11) and other cancer cell lines (n = 1008) using Cancer Cell Line Encyclopedia (CCLE) datasets. mRNA expression was indicated by Log_2 intensity and box plots. *P*-values were calculated by two-sided Mann-Whitney *U* test. B, Normalized *OXTR* mRNA expression across 25 tumor types from CCLE datasets showing high overall expression in MM cell lines (MM, red). C, Clinical and molecular characteristics of 87 MM cases from The Cancer Genome Atlas (TCGA) datasets. The 87 MM cases were divided into three groups according to *OXTR* mRNA expression level: low (n = 29), moderate (n = 29), and high groups (n = 29). D, Kaplan-Meier survival curves of 85 MM cases from the TCGA datasets stratified according to *OXTR* mRNA expression (low- [n = 28], moderate- [n = 29], and high-expression groups [n = 28]; $P < .001$, log-rank test). Two cases with unknown prognosis were excluded from the 87 MM cases of the TCGA datasets. A, B, The box and horizontal line in the box indicate the interquartile range and median. The whiskers extend from the ends of the box to the outermost data point that falls within the distances computed as follows: first quartile −1.5 × (interquartile range) or third quartile +1.5 × (interquartile range)

TABLE 1 Univariate and multivariable analysis of overall survival in MM cases from TCGA datasets (n = 85)[a]

	Univariate analysis			Multivariable analysis		
Variable	**HR**	**95% CI**	***P*[c]**	**HR**	**95% CI**	***P*[c]**
Sex						
Female	Reference			Reference		
Male	0.89	0.49-1.59	0.689	0.92	0.48-1.77	0.801
Age						
≤65 years	Reference			Reference		
>65 years	1.39	0.87-2.23	0.171	1.13	0.67-1.92	0.641
Histology						
Epithelioid	Reference			Reference		
Sarcomatoid or biphasic	2.03	1.21-3.41	0.008	2.03	1.13-3.66	0.018
Stage						
I	Reference			Reference		
II	0.63	0.26-1.51	0.301	0.99	0.40-2.44	0.979
III	0.76	0.36-1.59	0.462	0.88	0.39-1.95	0.747
IV	0.71	0.30-1.67	0.429	0.88	0.34-2.33	0.804
OXTR mRNA expression[b]	2.25	1.66-3.05	<0.001	2.2	1.60-3.07	<0.001

Abbreviations: CI, confidence interval; HR, hazard ratio; MM, malignant mesothelioma; OXTR, oxytocin receptor; TCGA, The Cancer Genome Atlas.

[a]Two cases with unknown prognosis were excluded from 87 MM cases of TCGA datasets.

[b]*OXTR* mRNA was converted by log_{10} and used for analysis as continuous variables.

[c]*P*-values were calculated by Wald test.

cell lines with low *OXTR* expression (Y-MESO-30 and NCI-H2452). Both MM cell lines transfected with *NF2* knockdown siRNA showed two to three times higher *OXTR* expression than those transfected with siRNA control (Figure 2B), indicating that *NF2* is involved in the negative regulation of *OXTR* expression in MM. Next, we explored the functional relevance of *OXTR* in MM cell lines. First, we conducted an OXT administration experiment on MM cell lines to determine whether OXT-OXTR signaling was involved in MM cell proliferation. Additional OXT treatment moderately increased proliferation of three MM cell lines with high *OXTR* expression (NCI-H2052, Y-MESO-27, and NCI-H2373), but no significant difference was found in the proliferation of MeT-5A cells and one MM cell line with low *OXTR* expression (NCI-H2452) (Figure 2C). Then, we conducted transient *OXTR* knockdown with synthetic oligonucleotides and obtained efficient knockdown in these cell lines (Figure 2D). Notably, *OXTR* knockdown significantly reduced proliferation in the three MM cell lines with high *OXTR* expression, whereas no significant difference was noted in MeT-5A and NCI-H2452 cells compared with the siRNA control (Figure 2E). These results indicated that OXT-OXTR signaling promotes proliferation of MM cell lines with high *OXTR* expression.

We conducted lentiviral shRNA knockdown in the three MM cell lines with high *OXTR* expression (NCI-H2052, Y-MESO-27, and NCI-H2373) to achieve persistent knockdown of *OXTR* in these cells and obtained highly efficient results (Figure S2). As expected, cell proliferation analyses in these cell lines showed a dramatic decrease in cell proliferation (Figure 3A). Furthermore, we analyzed cell cycle profiles in these three cell lines to elucidate the suppressive mechanisms involved in MM cell proliferation by *OXTR* knockdown. Flow cytometric analyses demonstrated that

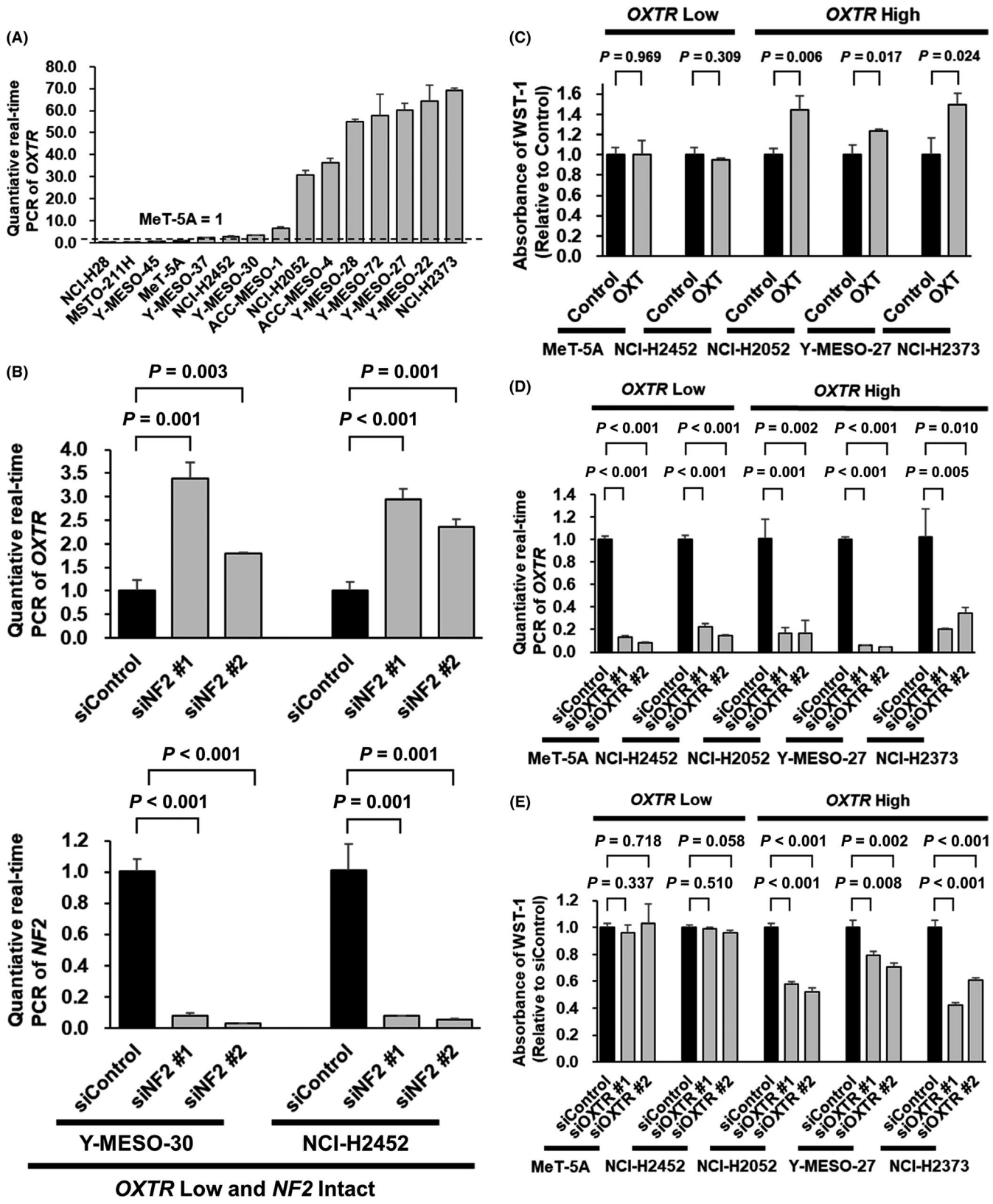

OXTR knockdown increased the G_1 phase fraction and decreased the G_2/M phase fraction in the three MM cell lines, indicating that *OXTR* downregulation disturbed tumor cell cycle mainly due to G_1 cell cycle arrest (Figure 3B). In addition, *OXTR* knockdown increased the sub-G_1 fraction in the three MM cell lines (Figure 3B). Based on the results of the cell cycle analyses, we investigated the expression levels of representative cell cycle–related genes, such as cyclins and cyclin-dependent kinases. In the three MM cell

FIGURE 2 The oxytocin–oxytocin receptor (OXT-OXTR) signaling promotes proliferation of malignant mesothelioma (MM) cell lines with high *OXTR* expression. A, qRT-PCR analysis of *OXTR* in 14 MM cell lines and MeT-5A (immortalized mesothelial cell line). *OXTR* mRNA expression of MeT-5A was used as a control (=1.0). *GAPDH* expression was used as a control. B, *Neurofibromin 2 (NF2)* knockdown using siRNA in Y-MESO-30 and NCI-H2452 was confirmed by qRT-PCR analysis. A significant increase in *OXTR* expression was observed in MM cell lines with *NF2* intact (Y-MESO-30 and NCI-H2452) treated with *NF2* siRNA compared with the siRNA control. C, Effect of OXT on cell proliferation in MeT-5A and four MM cell lines (NCI-H2452, NCI-H2052, Y-MESO-27, and NCI-H2373). Three days after treatment with 1 nM OXT, cell proliferation was analyzed in MM cell lines and MeT-5A cells by WST-1 colorimetric assay. D, *OXTR* knockdown using siRNA in MeT-5A cells and four MM cell lines (NCI-H2452, NCI-H2052, Y-MESO-27, and NCI-H2373) was confirmed by qRT-PCR analysis. E, WST-1 colorimetric assay 4 d after transient *OXTR* knockdown by *OXTR* siRNA and negative siRNA control in MeT-5A, NCI-H2452, NCI-H2052, Y-MESO-27, and NCI-H2373 cells. A significant reduction in cell proliferation was observed in MM cell lines with high *OXTR* expression (NCI-H2052, Y-MESO-27, and NCI-H2373) treated with *OXTR* siRNA. Data represent mean and standard deviation of triplicate samples from a representative experiment. All *P*-values were calculated using two-sided unpaired *t*-test

lines, *OXTR* knockdown significantly reduced the expression levels of *CCNE2*, *CDK2*, *CDK1*, and *AURKA*, but did not decrease those of *CCNE1* (Figure 3C), suggesting that *CCNE2*, *CDK2*, and *CDK1* downregulation induced G_1 cell cycle arrest, and *CDK1* and *AURKA* downregulations were associated with decreased G_2/M phase fraction.[28-30] Furthermore, we found a weak positive correlation between *CCNE2* or *CDK2* and *OXTR* mRNA expression and moderate positive correlations between *CDK1* or *AURKA* and *OXTR* mRNA expression in 87 MM cases in the TCGA dataset (Figure 3D). These results indicate that downstream signals from *OXTR* could promote MM cell proliferation through cell cycle regulation. Moreover, we investigated the role of *OXTR* in MM colony formation ability and found that *OXTR* knockdown significantly suppressed colony formation in cell lines with high *OXTR* expression (Figure 4A). In addition, wound-healing assay showed that *OXTR* knockdown significantly decreased the migration of MM cells with high *OXTR* expression (Figure 4B), suggesting that increased *OXTR* expression in MM could facilitate tumor progression. To assess the suppressive effect involved in MM progression by *OXTR* knockdown in vivo, we injected NCI-H2052/NCI-H2373 cells transfected with sh*OXTR* lentivirus or empty lentivirus into the subcutaneous space of nude mice. Four weeks after transplantation, the tumor weights of both *OXTR* knockdown groups were significantly reduced compared with the control groups (NCI-H2052: 37.0 vs. 14.0 mg, $P = .001$; NCI-H2373: 63.3 vs. 14.3 mg, $P = .004$) (Figure 4C). These results indicate that *OXTR* knockdown dramatically suppresses MM tumor progression and that *OXTR* could be a new promising therapeutic target in MM.

3.3 | *OXTR* antagonists inhibit MM progression

Our results led us to hypothesize that *OXTR* antagonists could have antitumor effects against MM cells with high *OXTR* expression. We used four *OXTR* antagonists (Table S4) to examine whether they could suppress MM cell proliferation in NCI-H2052, Y-MESO-27, and NCI-H2373 MM cell lines with high *OXTR* expression. All four *OXTR* antagonists showed inhibitory effects against MM cell proliferation (Figure 5A). Interestingly, the IC_{50} of the antagonists for the three MM cell lines showed a tendency toward a positive correlation with their inhibition constant (Ki) for *OXTR* (Figure 5A and Table S4). We selected two *OXTR* antagonists, atosiban (Ki for OXTR = 397 nM) and cligosiban (Ki for OXTR = 9.5 nM), to further investigate the cytostatic activity of *OXTR* antagonists. The IC50s of both *OXTR* antagonists were analyzed in MeT-5A cells, five MM cell lines with low *OXTR* expression, and five MM cell lines with high *OXTR* expression. As expected, cligosiban showed stronger cytostatic activity for MM cell lines than atosiban, and the average IC_{50} for the five MM cell lines with high *OXTR* expression was significantly lower than that of the five MM cell lines with low *OXTR* expression (30.2 vs. 63.1 μM; $P = .008$, Mann-Whitney U test) (Figure S3A, B, and Figure 5B). In addition, the IC_{50} of cligosiban was the highest for MeT-5A compared with all MM cell lines (Figure 5B). We examined the effect of cligosiban combined with cisplatin (CDDP), which is a standard chemotherapy agent in MM treatment. Cligosiban showed significant additive effects in combination with CDDP in the three MM cell lines with high *OXTR* expression, namely NCI-H2052, Y-MESO-27, and NCI-H2373 (Figure 5C). The clinical efficacy of cligosiban with oral administration was investigated in some clinical trials for men with premature ejaculation, and the rate of serious adverse events was extremely low.[31,32] Therefore, we further investigated the antitumor effects of orally administered cligosiban on MM using a xenograft model of NCI-H2052 (Figure 5D). Interestingly, the tumor weights after 10 doses of orally administered cligosiban were significantly reduced compared with those of the control group (29.0 vs. 56.8 mg; $P = .021$) (Figure 5E). Additionally, to determine whether cligosiban affected *OXTR* expression in MM cells, we repeated the experiment and found that there was no difference of *OXTR* expression between the treated and control groups (Figure S4A and B), suggesting that the antitumor effect of cligosiban is mainly exerted through the blockade of OXT to *OXTR*, but the *OXTR* expression is not affected. These results indicate that *OXTR* antagonists, which have high selectivity for OXTR, inhibit MM tumor progression and are new promising antitumor agents.

4 | DISCUSSION

To the best of our knowledge, this is the first study to show that *OXTR* expression is remarkably upregulated in MM compared with other tumor types and cases with high expression have worse clinical outcomes. *OXTR* knockdown dramatically suppressed cell

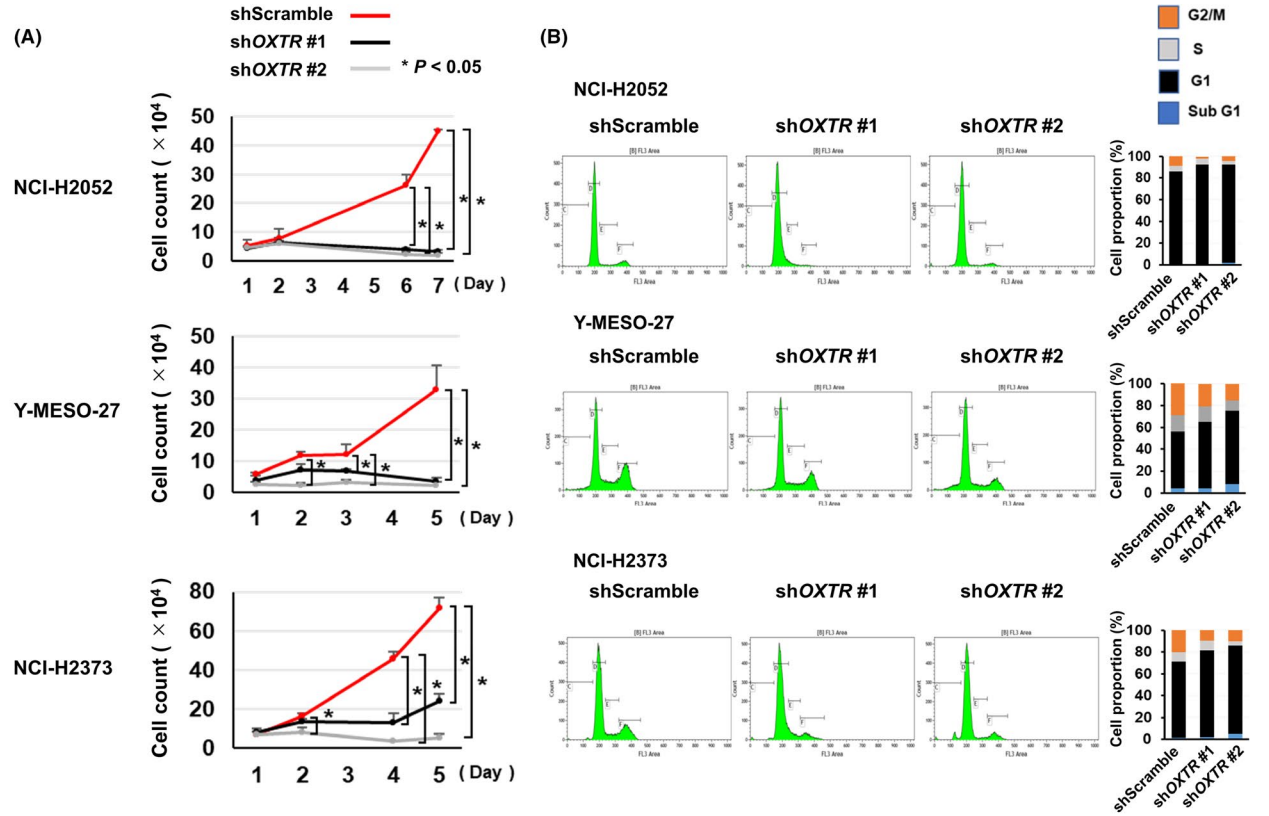
(A)
shScramble
shOXTR #1
shOXTR #2
* P < 0.05
NCI-H2052
Y-MESO-27
NCI-H2373
Cell count (×10⁴)
(Day)
(B)
G2/M
S
G1
Sub G1
shScramble
shOXTR #1
shOXTR #2
Cell proportion (%)

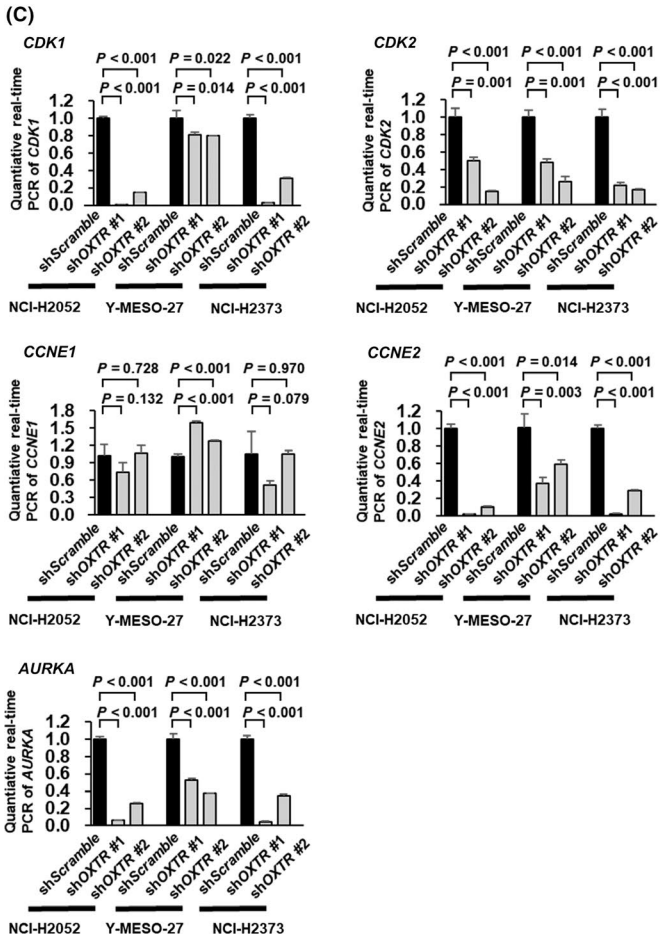
(C)
CDK1
CDK2
CCNE1
CCNE2
AURKA
Quantiative real-time PCR of CDK1
Quantiative real-time PCR of CDK2
Quantiative real-time PCR of CCNE1
Quantiative real-time PCR of CCNE2
Quantiative real-time PCR of AURKA
NCI-H2052
Y-MESO-27
NCI-H2373

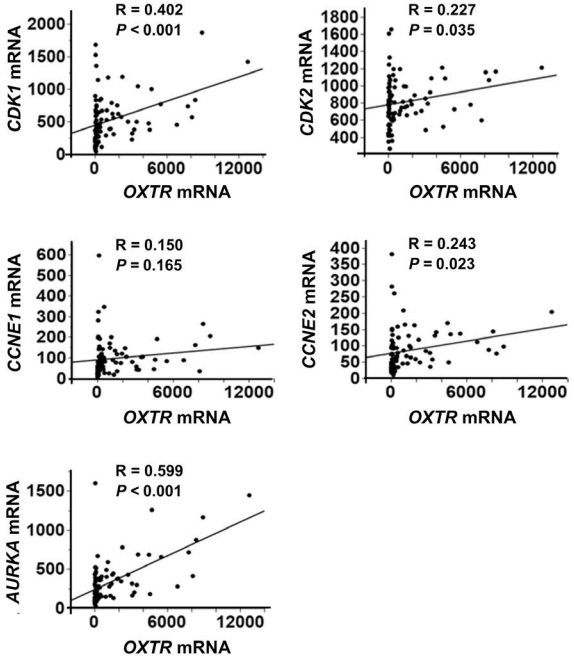
(D)
CDK1 mRNA
CDK2 mRNA
CCNE1 mRNA
CCNE2 mRNA
AURKA mRNA
OXTR mRNA
R = 0.402
P < 0.001
R = 0.227
P = 0.035
R = 0.150
P = 0.165
R = 0.243
P = 0.023
R = 0.599
P < 0.001

FIGURE 3 *Oxytocin receptor (OXTR)* knockdown disturbs tumor cell cycle in malignant mesothelioma (MM) cell lines with high *OXTR* expression. A, Cell proliferation analyses in MM cell lines with high *OXTR* expression (NCI-H2052, Y-MESO-27, and NCI-H2373) transfected with *OXTR*-knockdown lentivirus or control. *$P < .05$ (sh*OXTR* vs. control). B, Flow cytometric analyses in NCI-H2052, Y-MESO-27, and NCI-H2373 cells 5 d after transfection with *OXTR*-knockdown lentivirus or control. C, qRT-PCR analyses of cell cycle–related genes in three MM cell lines after infection with *OXTR*-knockdown lentivirus or control. *GAPDH* expression was used as a control. D, Correlation of mRNA expression levels of *OXTR* and cell cycle–related genes (*CDK1*, *CDK2*, *CCNE1*, *CCNE2*, and *AURKA*) in 87 MM tissues from The Cancer Genome Atlas (TCGA) datasets. Pearson correlation coefficient and *P*-values were calculated. All statistical tests were two-sided. A and C, Data represent mean and standard deviation of triplicate samples from a representative experiment. All *P*-values were calculated using two-sided unpaired *t*-test

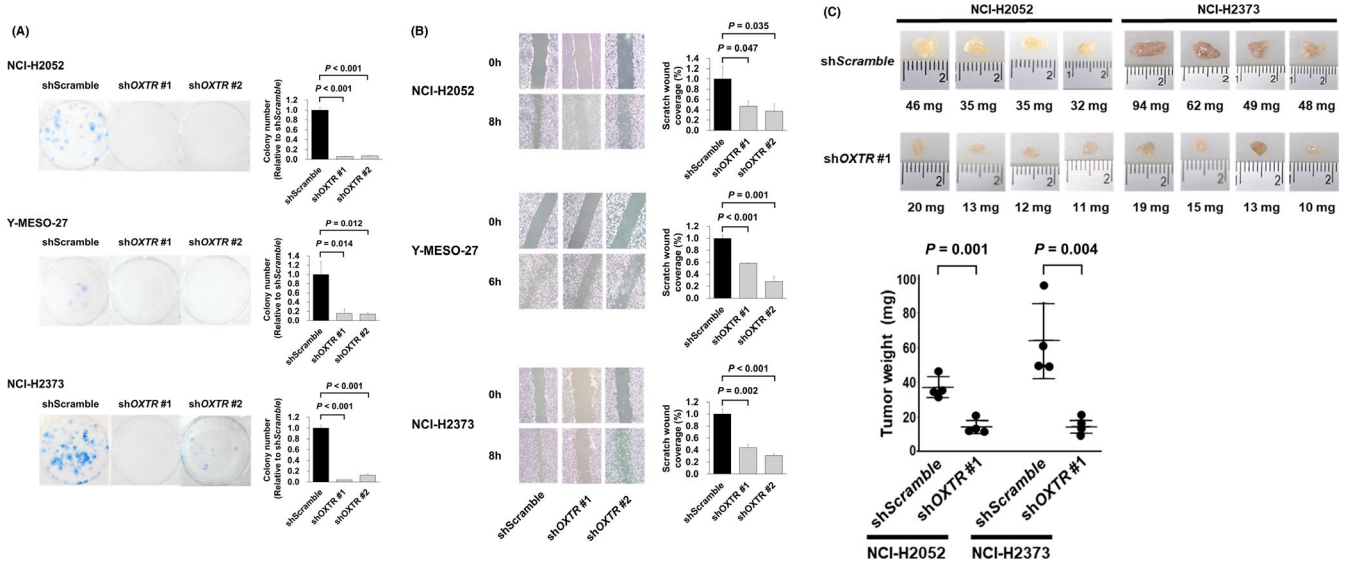

FIGURE 4 *Oxytocin receptor (OXTR)* knockdown suppresses malignant mesothelioma (MM) tumor progression. A, Colony formation assay in NCI-H2052, Y-MESO-27, and NCI-H2373 cells after infection with *OXTR*-knockdown lentivirus or control. Columns indicate the average of triplicate samples from a representative experiment, and bars indicate standard deviation. B, Cell migration abilities after persistent *OXTR* knockdown in NCI-H2052, Y-MESO- 27, and NCI-H2373 cells were analyzed by scratch wound–healing assay. Columns indicate the average of three different parts from a representative experiment, and bars indicate standard deviation. C, shScramble or sh*OXTR* #1 NCI-H2052/NCI-H2373 cells (1.5×10^6 cells/200 μL) were injected subcutaneously into BALB/c nude mice (shScramble group, n = 4; sh*OXTR* #1 group, n = 4). After 28 d, the tumor weights of the shScramble and sh*OXTR* #1 groups were measured. Horizontal lines indicate average and standard deviation. All *P*-values were calculated by two-sided unpaired *t*-test

proliferation of MM cell lines with high *OXTR* expression through disturbance of tumor cell cycle. *OXTR* antagonists significantly inhibited the growth of MM cell lines, and oral administration of the *OXTR* antagonist, cligosiban, suppressed MM tumor progression. *OXTR* could be a promising therapeutic target and a new prognostic indicator in MM.

In normal tissue, *OXTR* is predominantly expressed in the mammary gland and uterine myometrium at the end of pregnancy and plays important roles in the induction of milk ejection and uterine contraction.[20] *OXTR* is also present in the central nervous system and modulates various behaviors.[33,34] Thus, OXT secretion levels are known to be important in men and women.[35] At the end of pregnancy, *OXTR* expression is strikingly increased in the uterine myometrium for contraction, while OXT secretion levels do not significantly change.[20] Similarly, our analysis showed that *OXTR* expression was significantly increased in MM, while endogenous *OXT* expression in MM was not higher than that in other cancer types (Figure S5A-C). Thus, we hypothesized that *OXTR* upregulation plays crucial roles in MM progression without increasing OXT secretion. Several studies have reported that *OXTR* was associated with tumor progression in some cancer types, such as small cell lung carcinoma and prostate cancer.[36,37] However, the molecular mechanism of *OXTR* downstream in tumor promotion is not well understood. We showed that *OXTR* knockdown significantly suppressed proliferation of MM cell lines through an increase in the G_1 phase of the cell cycle. Furthermore, cell cycle arrest was caused by decreased expression levels of cyclin, cyclin-dependent kinases, and serine/threonine protein kinases, such as *CCNE2*, *CDK1*, *CDK2*, and *AURKA*. In particular, *CDK1* and *AURKA* were previously reported as potential therapeutic target genes in MM.[38,39] To further support this, expression levels of the four genes were positively correlated with *OXTR* expression in the TCGA dataset. These results indicate that *OXTR* upregulation promotes MM progression through cell cycle acceleration, although further studies are required to identify the mechanism involved in the downregulation of the four genes caused by *OXTR* knockdown.

In this study, *OXTR* antagonists were shown to have antitumor effects against MM cells with high *OXTR* expression, although the

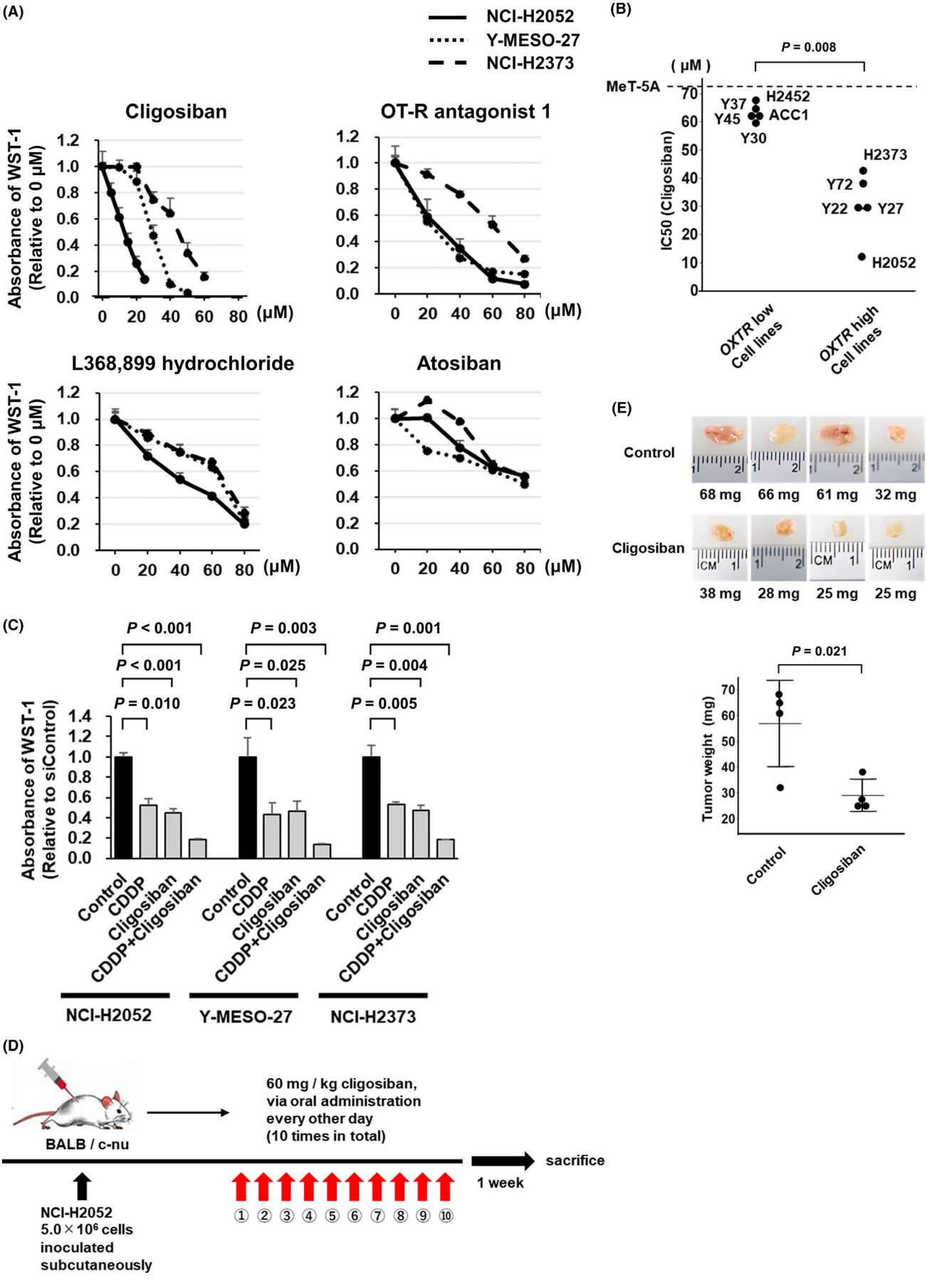
(A)
NCI-H2052
Y-MESO-27
NCI-H2373
Cligosiban
OT-R antagonist 1
L368,899 hydrochloride
Atosiban
Absorbance of WST-1 (Relative to 0 μM)
(μM)
(B)
P = 0.008
(μM)
MeT-5A
IC50 (Cligosiban)
Y37
H2452
Y45
ACC1
Y30
H2373
Y72
Y22
Y27
H2052
OXTR low Cell lines
OXTR high Cell lines
(E)
Control
Cligosiban
68 mg
66 mg
61 mg
32 mg
38 mg
28 mg
25 mg
25 mg
P = 0.021
Tumor weight (mg)
Control
Cligosiban
(C)
P < 0.001
P < 0.001
P = 0.010
P = 0.003
P = 0.025
P = 0.023
P = 0.001
P = 0.004
P = 0.005
Absorbance of WST-1 (Relative to siControl)
Control
CDDP
Cligosiban
CDDP+Cligosiban
NCI-H2052
Y-MESO-27
NCI-H2373
(D)
BALB / c-nu
60 mg / kg cligosiban,
via oral administration
every other day
(10 times in total)
sacrifice
1 week
NCI-H2052
5.0 × 10⁶ cells
inoculated
subcutaneously
① ② ③ ④ ⑤ ⑥ ⑦ ⑧ ⑨ ⑩

FIGURE 5 Oxytocin receptor (OXTR) antagonists inhibit malignant mesothelioma (MM) progression. A, WST-1 colorimetric assay in cell lines with high *OXTR* expression (NCI-H2052, Y-MESO-27, and NCI-H2373) cultured with various concentrations of four *OXTR* antagonists for 5 d. Data represent mean and standard deviation of triplicate samples from a representative experiment. B, IC_{50} of cligosiban for five MM cell lines with low *OXTR* expression, five MM cell lines with high *OXTR* expression, and MeT-5A cells (immortalized mesothelial cell line). *P*-values were calculated using two-sided Mann-Whitney U test (low vs. high *OXTR* expression in MM cell lines). Dashed line indicates the IC_{50} of cligosiban in MeT-5A cells. C, WST-1 colorimetric assay of MM cell lines with high *OXTR* expression (NCI-H2052, Y-MESO-27, and NCI-H2373) 5 d after treatment with cisplatin (CDDP) and/or cligosiban. CDDP or cligosiban was used at the IC_{50} for the respective cell lines as follows: NCI-H2052, 0.8 μM CDDP and 15 μM cligosiban; Y-MESO-27, 0.95 μM CDDP and 25 μM cligosiban; and NCI-H2373, 6 μM CDDP and 45 μM cligosiban. Columns indicate the average of triplicate samples from a representative experiment, and bars indicate standard deviation. D, Outline of the method used for the cligosiban oral administration experiment in a xenograft model. NCI-H2052 cells (5.0×10^6 cells/200 μL) were inoculated subcutaneously into BALB/c nude mice. After transplantation, dimethyl sulfoxide (DMSO) or cligosiban (60 mg/kg) was administered every other day via oral administration (control group, n = 4; cligosiban group: n = 4). DMSO or cligosiban were administered 10 times in total. E, Tumor weights were measured 1 wk after the last administration of DMSO or cligosiban. Horizontal lines indicate mean and standard deviation. C and E, All *P*-values were calculated by two-sided unpaired *t*-test

IC_{50} values of these drugs were relatively high. Atosiban has been clinically used in European countries as a treatment for preterm birth,[40] and its antitumor effects were reported in the human prostate cancer cell line DU145[41] although the selectivity for *OXTR* was relatively lower than the other antagonists (Table S4). Our analysis showed that the IC_{50} values of *OXTR* antagonists for MM cell lines tended to positively correlate with the Ki for OXTR. *OXTR* is known to be structurally similar to vasopressin receptors;[20] therefore, the selectivity for *OXTR* could be an important factor to use *OXTR* antagonists as antitumor agents. Developing new agents with a high selectivity for *OXTR* is essential to obtain *OXTR* antagonists with high antitumor effects against MM. However, the selectivity of cligosiban for *OXTR* is >100 times greater than for the vasopressin receptor, and the Ki is less than one-fortieth that of atosiban (Table S4). A phase IIb, randomized clinical trial using cligosiban was recently conducted in men with premature ejaculation and reported extremely low rate of adverse events.[31,32] Therefore, it may be possible to further increase the dose when we will clinically use cligosiban as an antitumor agent against MM. In our xenograft model, a total of 10 doses of cligosiban (60 mg/kg) were administered orally every other day and led to a significant reduction in tumor volume. This dose of cligosiban could be acceptable from the perspective of adverse events based on the findings of a previous clinical setting, although the dose was equivalent to almost the maximum setting of the trial.[42] A rigid and deformable dose setting would be necessary in a first clinical trial to examine the clinical efficacy of cligosiban against MM.

Molecular mechanisms that increase *OXTR* expression in MM were not completely identified in the present study. A previous study indicated that *OXTR* is transcriptionally regulated by interleukin (IL)-6 and IL-1β,[43] whereas administration of IL-6 or IL-1β in MM cell lines with low *OXTR* expression did not significantly increase *OXTR* mRNA expression (Figure S6). Analysis of driver gene inactivation using MM cell lines and TCGA datasets revealed that *OXTR* mRNA expression was statistically associated with *NF2* inactivation. Consistently, our experiment showed that *NF2* knockdown increased *OXTR* expression, indicating that *NF2* may be involved in negative regulation of the *OXTR* transcription. In this regard, *NF2* is involved in dysfunction of the Hippo signaling pathway, and inactivation of the NF2-Hippo pathway leads to continual activation of the transcriptional coactivator YAP1, which is a key molecule involved in MM progression, by translocating YAP1 from the cytoplasm to the nucleus.[18] Based on these findings, we also conducted *YAP1* knockdown using several MM cell lines; however, *OXTR* expression levels did not change remarkably (data not shown). Further studies are required to identify the regulatory mechanism involved in increased *OXTR* expression in MM. Regarding the clinical relevance of *OXTR* in MM, high *OXTR* expression was significantly associated with poor overall survival. Therefore, *OXTR* expression levels could be a promising molecular biomarker and could enable personalized treatment against MM. Patient selection based on immunohistochemical analysis or mRNA in situ hybridization is desirable to develop a new therapeutic strategy targeting high *OXTR* expression, and further analysis is necessary to establish the methods.

In conclusion, we identified high *OXTR* expression in MM, which was associated with poor overall survival. *OXTR* knockdown and administration of *OXTR* antagonists in vitro and in vivo experiments showed significant suppression of MM cell proliferation. These results indicate that *OXTR* could be a promising therapeutic target and a prognostic biomarker, enabling a personalized approach to treatment of MM.

ACKNOWLEDGMENTS

The authors would like to thank Enago (www.enago.jp) for the English language review and Yoshie Sato for her excellent technical assistance.

DISCLOSURE

Dr Hashimoto reported receiving grant from Boehringer Ingelheim; Pfizer Inc; Astellas Pharma Inc; Ono Pharmaceutical Co.; Shionogi & Co.; AstraZeneca; Sanofi KK; Teijin Limited; MSD KK; Meiji Seika Pharma Co.; Daiichi Sankyo Company, Limited; GlaxoSmithKline KK; Otsuka Pharmaceutical Co.; KYORIN Pharmaceutical Co., Ltd.; Sumitomo Dainippon Pharma Co.; Novartis Pharma KK; Kyowa Hakko Kirin Co.; Eli Lilly Japan KK; and Chugai Pharmaceutical Co. that was paid to Nagoya University. Other authors have no conflict of interest.

ORCID

Ichidai Tanaka https://orcid.org/0000-0002-5517-0598
Mitsuo Sato https://orcid.org/0000-0001-5458-9576
Naozumi Hashimoto https://orcid.org/0000-0003-2337-629X

REFERENCES

1. Scherpereel A, Wallyn F, Albelda SM, Munck C. Novel therapies for malignant pleural mesothelioma. *Lancet Oncol*. 2018;19:e161-e172.
2. Carbone M, Kratzke RA, Testa JR. The pathogenesis of mesothelioma. *Semin Oncol*. 2002;29:2-17.
3. Odgerel CO, Takahashi K, Sorahan T, et al. Estimation of the global burden of mesothelioma deaths from incomplete national mortality data. *Occup Environ Med*. 2017;74:851-858.
4. Rusch VW, Chansky K, Kindler HL, et al. The IASLC mesothelioma staging project: proposals for the M descriptors and for revision of the TNM stage groupings in the forthcoming (Eighth) edition of the TNM classification for mesothelioma. *J Thorac Oncol*. 2016;11:2112-2119.
5. Røe OD, Stella GM. Malignant pleural mesothelioma: history, controversy and future of a manmade epidemic. *Eur Respir Rev*. 2015;24:115-131.
6. Vogelzang NJ, Rusthoven JJ, Symanowski J, et al. Phase III study of pemetrexed in combination with cisplatin versus cisplatin alone in patients with malignant pleural mesothelioma. *J Clin Oncol*. 2003;21:2636-2644.
7. Ceresoli GL, Zucali PA, Favaretto AG, et al. Phase II study of pemetrexed plus carboplatin in malignant pleural mesothelioma. *J Clin Oncol*. 2006;24:1443-1448.
8. Highlights of prescribing information. www.fda.gov/medwatch. (accessed 29 Oct 2020)
9. Larkin J, Chiarion-Sileni V, Gonzalez R, et al. Five-year survival with combined nivolumab and ipilimumab in advanced melanoma. *N Engl J Med*. 2019;381:1535-1546.
10. Motzer RJ, Escudier B, McDermott DF, et al. Nivolumab versus everolimus in advanced renal-cell carcinoma. *N Engl J Med*. 2015;373:1803-1813.
11. Hmeljak J, Sanchez-Vega F, Hoadley KA, et al. Integrative molecular characterization of malignant pleural mesothelioma. *Cancer Discov*. 2018;8:1549-1565.
12. Bueno R, Stawiski EW, Goldstein LD, et al. Comprehensive genomic analysis of malignant pleural mesothelioma identifies recurrent mutations, gene fusions and splicing alterations. *Nat Genet*. 2016;48:407-416.
13. Carbone M, Harbour JW, Brugarolas J, et al. Biological mechanisms and clinical significance of BAP1 mutations in human cancer. *Cancer Discov*. 2020;10:1103-1120.
14. Sato T, Sekido Y. NF2/merlin inactivation and potential therapeutic targets in mesothelioma. *Int J Mol Sci*. 2018;19:988.
15. Tanaka I, Osada H, Fujii M, et al. LIM-domain protein AJUBA suppresses malignant mesothelioma cell proliferation via Hippo signaling cascade. *Oncogene*. 2013;34:73-83.
16. Huang J, Wu S, Barrera J, Matthews K, Pan D. The Hippo signaling pathway coordinately regulates cell proliferation and apoptosis by inactivating Yorkie, the Drosophila homolog of YAP. *Cell*. 2005;122:421-434.
17. Murakami H, Mizuno T, Taniguchi T, et al. LATS2 is a tumor suppressor gene of malignant mesothelioma. *Cancer Res*. 2011;71:873-883.
18. Badouel C, Garg A, McNeill H. Herding Hippos: regulating growth in flies and man. *Curr Opin Cell Biol*. 2009;21:837-843.
19. Mizuno T, Murakami H, Fujii M, et al. YAP induces malignant mesothelioma cell proliferation by upregulating transcription of cell cycle-promoting genes. *Oncogene*. 2012;31:5117-5122.
20. Gimpl G, Fahrenholz F. The oxytocin receptor system: structure, function, and regulation. *Physiol Rev*. 2001;81:629-683.
21. Lerman B, Harricharran T, Ogunwobi OO. Oxytocin and cancer: an emerging link. *World J Clin Oncol*. 2018;9:74-82.
22. Cassoni P, Sapino A, Marrocco T, Chini B, Bussolati G. Oxytocin and oxytocin receptors in cancer cells and proliferation. *J Neuroendocrinol*. 2004;16:362-364.
23. Kutner RH, Zhang XY, Reiser J. Production, concentration and titration of pseudotyped HIV-1-based lentiviral vectors. *Nat Protoc*. 2009;4:495-505.
24. Sanyal D, Kudesia G, Corbitt G. Comparison of ultracentrifugation and polyethylene glycol precipitation for concentration of hepatitis B virus (HBV) DNA for molecular hybridisation tests and the relationship of HBV-DNA to HBe antigen and anti-HBe status. *J Med Microbiol*. 1991;35:291-293.
25. Lo HL, Yee JK. Production of vesicular stomatitis virus G glycoprotein (VSV-G) pseudotyped retroviral vectors. *Curr Protoc Hum Genet*. 2007;Chapter 12:unit 12.7.
26. Marino MP, Luce MJ, Reiser J. Small- to large-scale production of lentivirus vectors. *Methods Mol Biol*. 2003;229:43-55.
27. Celiktas M, Tanaka I, Tripathi SC, et al. Role of CPS1 in cell growth, metabolism, and prognosis in LKB1-inactivated lung adenocarcinoma. *J Natl Cancer Inst*. 2017;109:1-9.
28. Carvajal RD, Tse A, Schwartz GK. Aurora kinases: new targets for cancer therapy. *Clin Cancer Res*. 2006;12:6869-6875.
29. Gudas JM, Payton M, Thukral S, et al. Cyclin E2, a novel G1 cyclin that binds Cdk2 and is aberrantly expressed in human cancers. *Mol Cell Biol*. 1999;19:612-622.
30. Enserink JM, Kolodner RD. An overview of Cdk1-controlled targets and processes. *Cell Div*. 2010;5:11.
31. Althof S, Osterloh IH, Muirhead GJ, et al. The oxytocin antagonist cligosiban fails to prolong intravaginal ejaculatory latency in men with lifelong premature ejaculation: results of a randomized, double-blind, placebo-controlled phase IIb trial (PEDRIX). *J Sex Med*. 2019;16:1188-1198.
32. McMahon C, Althof S, Rosen R, et al. The oxytocin antagonist cligosiban prolongs intravaginal ejaculatory latency and improves patient-reported outcomes in men with lifelong premature ejaculation: results of a randomized, double-blind, placebo-controlled proof-of-concept trial (PEPIX). *J Sex Med*. 2019;16:1178-1187.
33. Gregory SG, Connelly JJ, Towers AJ, et al. Genomic and epigenetic evidence for oxytocin receptor deficiency in autism. *BMC Med*. 2009;7:1-13.
34. Horie K, Inoue K, Suzuki S, et al. Oxytocin receptor knockout prairie voles generated by CRISPR/Cas9 editing show reduced preference for social novelty and exaggerated repetitive behaviors. *Horm Behav*. 2019;111:60-69.
35. Leake RD, Weitzman RE, Glatz TH, Fisher DA. Plasma oxytocin concentrations in men, nonpregnant women, and pregnant women before and during spontaneous labor. *J Clin Endocrinol Metab*. 1981;53:730-733.
36. Péqueux C, Breton C, Hendrick JC, et al. Oxytocin synthesis and oxytocin receptor expression by cell lines of human small cell carcinoma of the lung stimulate tumor growth through autocrine/paracrine signaling. *Cancer Res*. 2002;62:4623-4629.
37. Zhong M, Boseman ML, Millena AC, Khan SA. Oxytocin induces the migration of prostate cancer cells: Involvement of the Gi-coupled signaling pathway. *Mol Cancer Res*. 2010;8:1164-1172.
38. Crispi S, Fagliarone C, Biroccio A, et al. Antiproliferative effect of Aurora kinase targeting in mesothelioma. *Lung Cancer*. 2010;70:271-279.
39. Linton A, Cheng YY, Griggs K, et al. An RNAi-based screen reveals PLK1, CDK1 and NDC80 as potential therapeutic targets in malignant pleural mesothelioma. *Br J Cancer*. 2014;110:510-519.
40. Lamont CD, Jørgensen JS, Lamont RF. The safety of tocolytics used for the inhibition of preterm labour. *Expert Opin Drug Saf*. 2016;15:1163-1173.
41. Reversi A, Rimoldi V, Marrocco T, et al. The oxytocin receptor antagonist atosiban inhibits cell growth via a 'biased agonist' mechanism. *J Biol Chem*. 2005;280:16311-16318.
42. Muirhead GJ, Osterloh IH, Whaley S, van den Berg F. Pharmacokinetics, safety, and tolerability of multiple doses of the novel oxytocin receptor antagonist cligosiban in development for premature ejaculation: two randomized clinical trials in healthy subjects. *J Sex Med*. 2019;16:213-222.

43. Schmid B, Wong S, Mitchell BF. Transcriptional regulation of oxytocin receptor by interleukin-1β and interleukin-6. *Endocrinology*. 2001;142:1380-1385.

SUPPORTING INFORMATION

Additional supporting information may be found online in the Supporting Information section.

How to cite this article: Kodama Y, Tanaka I, Sato T, et al. Oxytocin receptor is a promising therapeutic target of malignant mesothelioma. *Cancer Sci*. 2021;112:3520–3532. https://doi.org/10.1111/cas.15025